

InAlN underlayer for near ultraviolet InGaN based light emitting diodes

Camille Haller^{*1}, Jean-François Carlin¹, Mauro Mosca^{1,2}, Marta D. Rossell³, Rolf Erni³, and Nicolas Grandjean¹

¹*Institute of Physics, Ecole Polytechnique Fédérale de Lausanne, Switzerland*

²*DEIM, University of Palermo, Italy*

³*Electron Microscopy Center, Empa, Swiss Federal Laboratories for Materials Science and Technology, Switzerland*

We report on InAlN underlayer (UL) to improve the efficiency of near ultraviolet (NUV) light emitting diodes (LEDs). While InGaN UL is commonly used in high efficiency blue LEDs it may absorb light for shorter wavelengths. InAlN lattice-matched to GaN exhibits a bandgap of 4.6 eV. This allows alleviating absorption issues in NUV LEDs. We demonstrate that the internal quantum efficiency of 405 nm single InGaN/GaN quantum well LEDs with InAlN UL is ~70% compared to less than 10% for LEDs without UL. Excellent I-V characteristics are achieved thanks to polarization charge screening with high doping level at InAlN/GaN interface.

Blue light emitting diodes (LEDs) based on III-nitride materials are used in many application nowadays and can reach internal quantum efficiency over 90%.¹ A closer look at the LED structure reveals the presence of an InGaN underlayer (UL) underneath the InGaN/GaN quantum well (QW) active region.²⁻⁴ The actual mechanism supporting the use of an InGaN UL is still debated in the literature. We recently proposed that indium atoms react with surface defects (SDs), resulting in their incorporation in the UL.^{4,5} Otherwise, those defects would have been incorporated in the InGaN/GaN QWs, reducing thereby their efficiency due to the concomitant introduction of non-radiative recombination centers (NRCs).⁵ We also demonstrated that In atoms are the key ingredient, since they efficiently capture SDs.⁵ Therefore, InAlN is a desirable material due to the high In content (17%) for lattice-matched (LM) condition to GaN.⁵ A schematic view of the role of the InAlN UL mechanism is depicted in Fig. 1. SDs are present at the surface after the high-temperature (HT) GaN buffer layer growth, (Fig. 1a). They segregate at the surface even for low temperature (LT) GaN growth, (Fig. 1b). Then, SDs are incorporated in InGaN QW layers due to a reaction with indium atoms creating NRCs, (Fig.

1c). The role of the InAlN UL is thus to trap SDs, (Fig. 1d), leading to defect-free InGaN/GaN QWs,

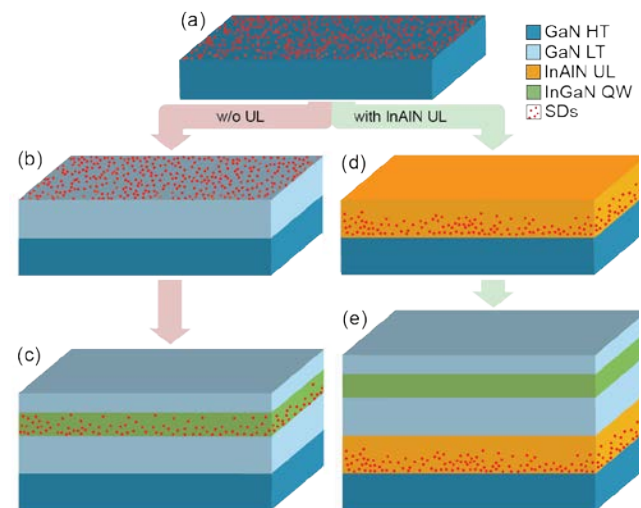


Figure 1: (a) Surface defects (SDs) are formed during GaN growth at high temperature. (b) These defects strongly segregate even during low temperature growth of GaN. (c) SDs react with In atoms and are eventually trapped in the InGaN QW where they create non-radiative recombination centers. (d) InAlN underlayer in which SDs are trapped due to their interaction with In atoms. (e) After the InAlN underlayer, the GaN surface is free of defects leading to high-efficiency InGaN/GaN QW.

(Fig 1e).

InGaN UL works perfectly in blue LEDs, as testified by their impressive performance. In the

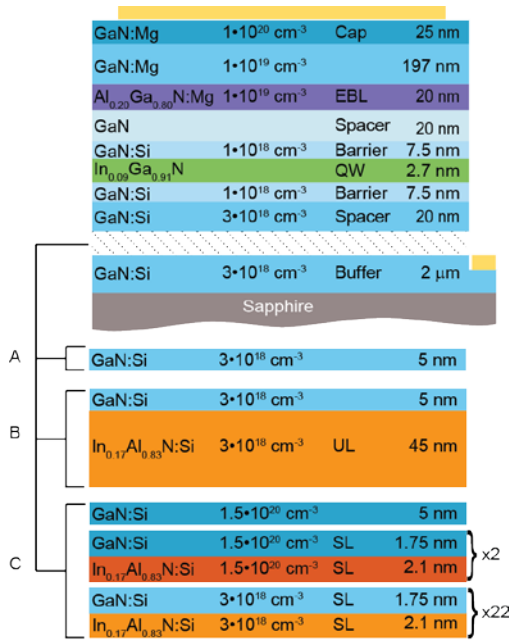


Figure 2: sketch of NUV SQW-LEDs with various epilayer structures: without UL (A), with InAlN bulk UL (B), and with InAlN/GaN SL UL (C).

case of near ultraviolet (NUV) LEDs, light absorption in the InGaN UL could become significant and affect the external efficiency of the devices. This could be alleviated by reducing the In composition in the UL. However, as the trapping of SDs directly depends on the total amount of In atoms, one would need a very thick InGaN layer.⁵ Such a thick UL may cause a degradation of the surface morphology and result in longer growth times. For instance, setting the In composition to 0.5% would require 450 nm thick InGaN UL to incorporate all SDs.⁵ An alternative, and attractive, solution is to move to an InAlN UL, since it would ensure transparency in NUV range with a bandgap of ~ 4.6 eV for LM condition.⁶ Also the thickness could be strongly reduced thanks to the high In content.

In this paper, we demonstrate that a thin (50 nm) InAlN UL strongly improves the efficiency of NUV (~ 405 nm) single (S)-QW LEDs. We also show that an InAlN/GaN short-period superlattice (SL) allows for excellent I-V characteristics.

The LED samples are grown in an Aixtron 200/4 RF-S metalorganic vapor phase epitaxy (MOVPE) reactor. Figure 2 depicts the different sample structures. The substrate is c-plane sapphire. After a LT GaN buffer, 2 μm of GaN is deposited at 1000°C using trimethylgallium (TMGa) with H_2 as a carrier gas. Then, the temperature is decreased to 770°C, and the carrier gas switched to N_2 for the growth of the $\text{In}_{0.17}\text{Al}_{0.83}\text{N}$ (bulk or SL), using trimethylindium (TMIn) and trimethylaluminum (TMAI). A 20 nm GaN spacer is grown at the same temperature with triethylgallium (TEGa) and with Si doping around $1 \cdot 10^{18} \text{ cm}^{-3}$. The InGaN/SQW is 2.7 nm thick and the In content 9%. It is capped by an undoped GaN spacer. Then the carrier gas is switched back to H_2 , and the temperature raised to 1000°C for the growth of the p -type layers. The latter consists of 20 nm $\text{Al}_{0.2}\text{Ga}_{0.8}\text{N:Mg}$ electron-blocking layer, 200 nm GaN:Mg layer, and 25 nm p^+ contact layer.

Three samples are compared: a reference sample without InAlN UL (Fig.2, structure A), a sample with 50 nm-thick bulk InAlN UL (Fig.2, structure B), and last one with 24x InAlN(2.1 nm)/GaN(1.75 nm) SL UL (Fig.2, structure C). Note that the total thickness of $\text{In}_{0.17}\text{Al}_{0.83}\text{N}$ in the SL corresponds to 50 nm, which is equivalent to the thickness of the bulk InAlN UL. This is aimed at incorporating the same amount of SDs.⁵ The samples were processed into $300 \times 300 \mu\text{m}^2$ LEDs with Ti/Al/Ti/Au stack layer for the n -type contact and Pd/Au for the p -type contact. The I-V characteristics reported later on correspond to our most significant data set. The electroluminescence intensity of the LEDs was recorded on wafer with a calibrated photodiode placed at the backside of the devices. The external quantum efficiency (EQE) was computed from the L-I curve. The maximum IQE was determined from raw data based on the method proposed by Dai *et al.*⁷ and Titkov *et al.*⁸

LEDs without UL exhibit a maximum IQE of $9\% \pm 5\%$ at a current density of 280 A/cm^2 . In contrast, devices featuring an InAlN bulk UL have a maximum IQE of $21\% \pm 5\%$ at a current density

of 110 A/cm^2 , (Fig. 3a). Thus, adding an InAlN UL increases the efficiency of the InGaN/GaN SQW, however the gain is moderate. One reason could be the InAlN material quality, which rapidly degrades when increasing the thickness.^{9–11} Especially V-pits could form and affect the overall performance of the

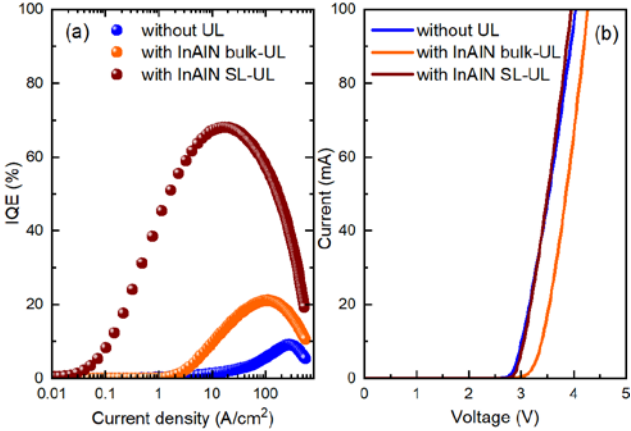


Figure 3: (a) IQE as a function of the current density for LEDs with structure A (blue), B (orange) and C (brown). (b) Current as function of the forward voltage for each LED type. The emission wavelength of those LEDs is $\sim 405 \text{ nm}$ and the device size is $300 \times 300 \mu\text{m}^2$.

devices. In order to keep a smooth surface and a high structural quality, the InAlN bulk layer was replaced by an InAlN/GaN SL.

Another potential drawback of InAlN UL deals with the I-V characteristics of LEDs. As shown in Fig. 3b, the turn-on voltage is increased by about 0.1 V on bulk InAlN UL LEDs compared to reference LEDs, i.e. 3.26 V and 3.16 V at 20 mA, respectively. This increase is attributed to the spontaneous polarization mismatch at the second InAlN/GaN interface. This leads to a negative fixed charge density of $\sim 2 \cdot 10^{13} \text{ cm}^{-2}$, which creates a barrier for electrons. To alleviate this electrostatic barrier, we introduced very high Si doping levels ($> 1 \cdot 10^{20} \text{ cm}^{-3}$) into the layers close to the interface, see Fig.2, structure C.

Scanning transmission electron microscopy (STEM) and energy dispersive x-ray (EDX) analysis were performed on the $24 \times \text{InAlN}(2.1 \text{ nm})/\text{GaN}(1.7 \text{ nm})$ SL UL LED sample. The results are shown in Fig. 4. The SL is clearly visible with sharp

interfaces between InAlN and GaN layers (Fig. 4a). Interestingly, the last two periods, which are over-doped with Si, have less defined interfaces. The EDX profile clearly shows intermixing between InAlN and GaN, see Fig. 4b. Notice that the effect of Si impurities on layer intermixing has already been observed in AlN/AlGaIn SL¹² and other semiconductor materials.^{13,14}

The I-V characteristics of InAlN/GaN SL UL NUV LEDs are comparable to those measured on reference LEDs (Fig. 3b). The voltage at 20 mA is 3.18 V and 3.16 V, respectively.

The maximum IQE of NUV SQW LEDs with an InAlN/GaN SL UL is $68\% \pm 5\%$ for a current density of 16 A/cm^2 , see Fig. 3. This is a significant improvement (about 8× more) over the reference LEDs. Combined with excellent I-V characteristics, this validates InAlN as a suitable material to trap SDs and increase the efficiency of InGaN/GaN QWs.

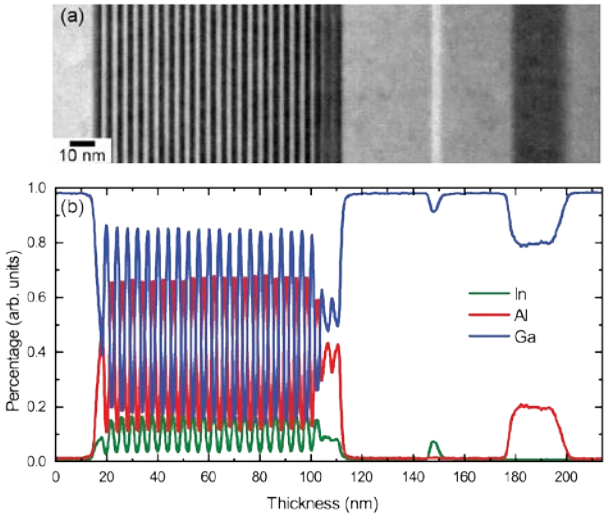


Figure 4: (a) Annular dark-field STEM image of the LED sample with an InAlN/GaN SL UL (structure C). (b) Corresponding In, Al, Ga composition profiles

In conclusion, we demonstrated that InAlN can act as an efficient UL for InGaN/GaN LEDs. This allows increasing the IQE without introducing any loss thanks to the large bandgap. This might be a key asset for NUV LEDs in the 370-410 range. We also show that an UL made of a short-period InAlN/GaN SL is superior to a bulk InAlN layer.

Finally, excellent I-V characteristics can be achieved provided that a high doping level is introduced at the InAlN/GaN interface in order to compensate the polarization-induced charges. The large band gap of InAlN UL opens new device designs for NUV InGaN based optoelectronics.

¹ A. David, C.A. Hurni, R.I. Aldaz, M.J. Cich, B. Ellis, K. Huang, F.M. Steranka, and M.R. Krames, *Applied Physics Letters* **105**, 231111 (2014).

² T. Akasaka, H. Gotoh, Y. Kobayashi, H. Nakano, and T. Makimoto, *Applied Physics Letters* **89**, 101110 (2006).

³ A.M. Armstrong, B.N. Bryant, M.H. Crawford, D.D. Koleske, S.R. Lee, and J.J. Wierer, *Journal of Applied Physics* **117**, 134501 (2015).

⁴ C. Haller, J.-F. Carlin, G. Jacopin, D. Martin, R. Butté, and N. Grandjean, *Applied Physics Letters* **111**, 262101 (2017).

⁵ C. Haller, J.-F. Carlin, G. Jacopin, W. Liu, D. Martin, R. Butté, and N. Grandjean, *Applied Physics Letters* **113**, 111106 (2018).

⁶ R. Butté, J.-F. Carlin, E. Feltn, M. Gonschorek, S. Nicolay, G. Christmann, D. Simeonov, A. Castiglia, J. Dorsaz, H.J. Buehlmann, S. Christopoulos, G. Baldassarri Höger von Hög, A.J.D. Grundy, M. Mosca, C. Pinquier, M.A. Py, F. Demangeot, J. Frandon, P.G. Lagoudakis, J.J.

Baumberg, and N. Grandjean, *Journal of Physics D: Applied Physics* **40**, 6328 (2007).

⁷ Q. Dai, Q. Shan, J. Wang, S. Chhajed, J. Cho, E.F. Schubert, M.H. Crawford, D.D. Koleske, M.-H. Kim, and Y. Park, *Applied Physics Letters* **97**, 133507 (2010).

⁸ I.E. Titkov, S.Y. Karpov, A. Yadav, V.L. Zerova, M. Zulonas, B. Galler, M. Strassburg, I. Pietzonka, H. Lugauer, and E.U. Rafailov, *IEEE Journal of Quantum Electronics* **50**, 911 (2014).

⁹ L. Yun, T. Wei, J. Yan, Z. Liu, J. Wang, and J. Li, *Journal of Semiconductors* **32**, 093001 (2011).

¹⁰ Ž. Gačević, S. Fernández-Garrido, J.M. Rebled, S. Estradé, F. Peiró, and E. Calleja, *Applied Physics Letters* **99**, 031103 (2011).

¹¹ G. Perillat-Merceroz, G. Cosendey, J.-F. Carlin, R. Butté, and N. Grandjean, *Journal of Applied Physics* **113**, 063506 (2013).

¹² J.J. Wierer, A.A. Allerman, and Q. Li, *Applied Physics Letters* **97**, 051907 (2010).

¹³ W.P. Gillin, I.V. Bradley, L.K. Howard, R. Gwilliam, and K.P. Homewood, *Journal of Applied Physics* **73**, 7715 (1993).

¹⁴ N. Bologna, S. Wirths, L. Francaviglia, M. Campanini, H. Schmid, V. Theofylaktopoulos, K.E. Moselund, A. Fontcuberta i Morral, R. Erni, H. Riel, and M.D. Rossell, *ACS Applied Materials & Interfaces* **10**, 32588 (2018).